www.sciencemag.org/cgi/content/full/1133599/DC1

Supporting Online Material for

Dynamical Configuration of Binary Near-Earth Asteroid (66391) 1999 KW4

D. J. Scheeres,* E. G. Fahnestock, S. J. Ostro, J.-L. Margot, L. A. M. Benner, S. B. Broschart, J. Bellerose, J. D. Giorgini, M. C. Nolan, C. Magri, P. Pravec, P. Scheirich, R. Rose, R. F. Jurgens, E. M. De Jong, S. Suzuki

*To whom correspondence should be addressed. E-mail: scheeres@umich.edu

Published 12 October 2006 on *Science* Express
DOI: 10.1126/science.1133599

This PDF file includes:

Other Supporting Online Material for this manuscript includes the following:
(available at www.sciencemag.org/cgi/content/full/1133599/DC1)

SUPPLEMENT: Dynamical Configuration of Binary Near-Earth Asteroid (66391) 1999 KW4

D. J. Scheeres,[1*] E. G. Fahnestock,[1] S. J. Ostro,[2] J.-L. Margot,[3]
L. A. M. Benner,[2] S. B. Broschart,[1] J. Bellerose,[1] J. D. Giorgini,[2]
M. C. Nolan,[4] C. Magri,[5] P. Pravec,[6] P. Scheirich,[6]
R. Rose,[2] R. F. Jurgens,[2] E. M. De Jong,[2] S. Suzuki,[2]

[1]Department of Aerospace Engineering, The University of Michigan,
1320 Beal Avenue, Ann Arbor, MI 48109-2140
[2]Jet Propulsion Laboratory, California Institute of Technology,
4800 Oak Grove Dr., Pasadena, CA 91109-8099
[3]Department of Astronomy, Cornell University,
610 Space Sciences Building, Ithaca, NY 14853
[4]Arecibo Observatory, HC03 Box 53995 Arecibo, Puerto Rico 00612
[5] Department of Natural Sciences, University of Maine at Farmington
173 High St, Farmington, ME 04938
[6] Astronomical Institute, Academy of Sciences of the Czech Republic
Fričova 1, CZ-25165 Ondřejov, Czech Republic
*To whom correspondence should be addressed; E-mail: scheeres@umich.edu.

Dynamics of the KW4 System

Simulation equations and model computation

The specific equations of motion solved for our simulations are stated in a compact form as (*1*):

$$
\begin{aligned}
m\ddot{r}_i &= U_{r_i} && (1)\\
\dot{H}^I_i &= -T^I_{ij}\epsilon_{jkl}T^I_{mk}U_{T^I_{ml}} && (2)\\
\Omega^I_i &= (I^I_{ji})^{-1}T^I_{kj}H^I_k && (3)\\
\dot{T}^I_{ij} &= T^I_{ik}\Omega^I_l\epsilon_{klj} && (4)\\
U(r,T^1,T^2) &= \mathcal{G}\int_{B^1}\int_{B^2}\frac{dm^1dm^2}{|r+T^1\rho^1-T^2\rho^2|} && (5)
\end{aligned}
$$

Here r is the relative position vector between the two centers of mass expressed in an inertial frame, the system mass parameter m equals the product of body masses divided by their sum, H^I is the inertial frame angular momentum vector of the Ith body, I^I is the inertia tensor of body I in its body-fixed frame, Ω^I is its angular velocity vector, T^I_{ij} is the attitude matrix of body I mapping its body-fixed frame to the inertial frame, ϵ_{ijk} is the skew-symmetric 3-tensor (with $\epsilon_{123}=1$) that defines the cross product, $\mathcal{G}$ is the universal constant of gravitation, B^I signifies the mass distribution of the body with differential mass element dm^I, ρ^I is the location of that mass element in the Ith body frame, and U is the mutual gravitational potential between the bodies. Dots over a variable denote time derivatives, subscripts on all variables except U denote vector, matrix or tensor elements, and we assume the Einstein summation convention. A subscript on U denotes partial differentiation.

To carry out one mutual potential evaluation for the mutual potential formulation(*2*) for two bodies with N and M facets requires NM operations. Using a conventional, high-order Runge-Kutta integration method for propagation of the system can add up to 13 additional potential, force, and moment evaluations per time step, albeit with an increase in the time step. On average, the Lee et al. (*3*) integrator provides an order of magnitude speed up in the simulation, as compared to a Runge-Kutta integration. The use of a parallel computer yields a two order of magnitude speed up. These techniques made it feasible to propagate the full KW4 simulation for time spans of months with a few weeks of computer time.

The dynamics of the KW4 system have been visualized with a computer animation that covers a two week time period. In this animation the relative orbit is excited to the point where the Beta libration angle reaches 8 degrees at maximum and the mutual obliquity of the system set at 10 degrees.

Angular Momentum Dynamics

The dynamics of the orbit and Alpha angular momentum vectors have a regularity that can be described with classical mechanics. Let the total angular momentum vector define the inertial frame's z-axis, and let the obliquity δ and the inclination i be the angles between the Alpha and orbit angular momentum vectors and the z-axis, respectively. Then due to Beta's on-average synchronous motion and Alpha's modest equatorial ellipticity, the respective magnitudes H and G of the Alpha and the orbit angular momentum vectors are constant on average, and constancy of the total angular momentum K

dictates the following relations:

$$K = H\cos\delta + G\cos i \quad (6)$$

$$H\sin\delta = G\sin i \quad (7)$$

The inclination and obliquity have only small fluctuations from their initial values, so the angular momentum vectors trace out cones in inertial space. Figure S1 shows the inclination and obliquity angles for various initial offsets between these vectors, integrated for fully interacting models with 100 facets each (to speed computation) over a one-year time span. The total angular momentum for a given initial condition pierces the center of each circle. The projected inclination and obliquity variations are displaced vertically to allow for clear distinctions between them.

Tidal Evolution

We computed timescales appropriate for the 1999 KW4 system under idealized assumptions mentioned in the text to find Fig. S4. This estimate should be viewed with considerable caution, because it is not clear that the tidal response of a gravitationally bound aggregate can be described realistically by two idealized numbers, and there is much uncertainty about the likely values of those numbers in the low-pressure, low-gravity regimes that have not been sampled in the laboratory. Furthermore, there may have been considerable evolution in the packing arrangement of KW4's constituent particles and hence in its response to tides at various epochs since its formation. Additional work is needed to understand the tidal response of rubble piles.

Implications for future missions

The expected presence of dynamical variation implies that a period of concerted ground-based or in-situ observations of KW4 could constrain the components' internal mass distributions by monitoring the system's time-varying behavior. Specifically, the low degree and order gravity field coefficients of the bodies can be inferred by observing the precession of the mutual orbit and the moments of inertia can be inferred by observing the system's time-varying rotational motion (*4*). Such a ground-based observation opportunity for KW4 will occur in 2018-2019.

If visited by a spacecraft, in addition to high resolution in situ observations there are several more aggressive observational techniques that are uniquely suited to a binary system with similar characteristics to KW4. An impact or explosion precipitated on Alpha's equator would provide profound insight into the composition of the regolith band at the equator. It would liberate large quantities of material, which would subsequently be size-sorted by solar radiation pressure and distributed throughout the binary system. Delivery of an inertial measurement unit on Beta would allow for precise determination of its time varying spin rate and motion, and could detect internal shifts in its mass distribution. Such measurements would enable precise determination of the system's mass distribution and would provide insight into the internal structure and mechanical properties of the bodies.

References and Notes

S1. A.J. Maciejewski. 1995. "Reduction, relative equilibria and potential in the two rigid bodies problem," *Celestial Mechanics & Dynamical Astronomy* 63(1):1 – 28.

S2. R.A. Werner and D.J. Scheeres. 2005. "Mutual potential of homogenous polyhedra," *Celestial Mechanics and Dynamical Astronomy* 91(3-4): 337-349.

S3. T. Lee, M. Leok, and N. H. McClamroch. 2005. "Lie group variational integrators for the Full Body Problem," *Computer Methods in Applied Mechanics and Engineering* Submitted. Available: `http://arxiv.org/abs/math.NA/0508365`

S4. D.J. Scheeres, J. Bellerose, E. Fahnestock "Missions to Binary Asteroids: Tra jectory Design, Navigation and Science," paper presented at the 6th International Astronautics Academy International Conference on Low-Cost Planetary Missions, Kyoto, Japan, (2005).

Figures

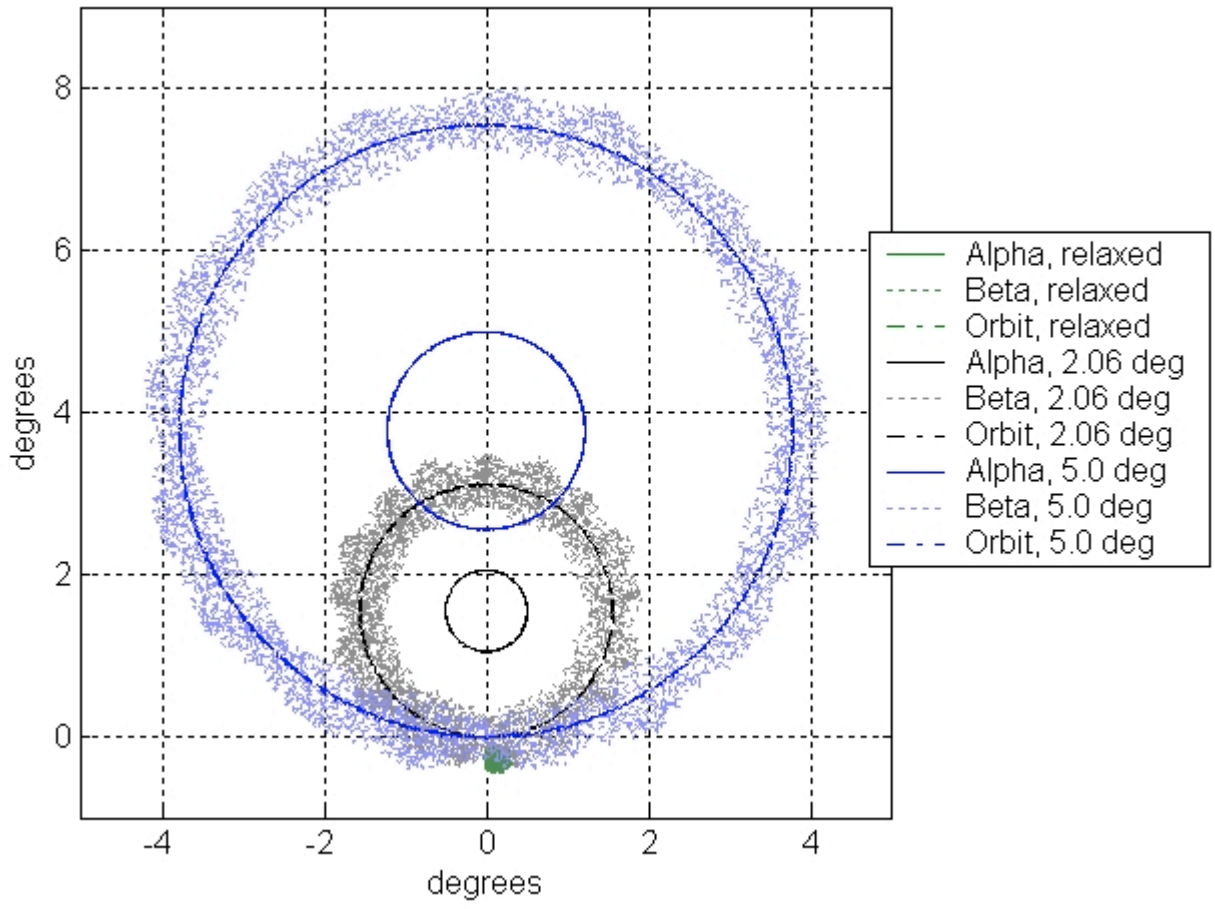
8
6
4
2
0
degrees
-4
-2
0
2
4
degrees
Alpha, relaxed
Beta, relaxed
Orbit, relaxed
Alpha, 2.06 deg
Beta, 2.06 deg
Orbit, 2.06 deg
Alpha, 5.0 deg
Beta, 5.0 deg
Orbit, 5.0 deg

a)

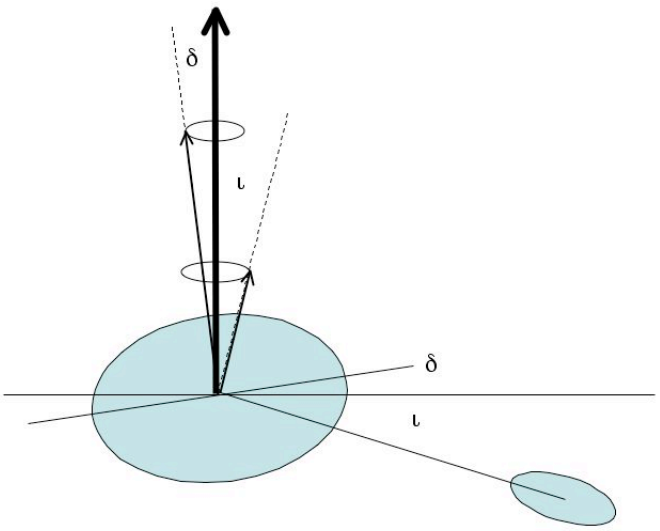

b)

Figure S1: (a) Projections of the orbit, Alpha and Beta angular momentum vectors onto an inertial plane, showing relaxed and excited angular momentum cases with the offset angle Δ equal to 0, 2, and 5°. Beta's angular momentum is always close to the orbit's and Alpha's angular momentum is always diametrically opposed to it. For each offset angle, the total angular momentum vector is at the center of the concentric circles. The radius of the orbit circle equals the inclination, i, and the radius of the Alpha circle equals the obliquity, δ. (b) The diagram shows the path followed by the evolving angular momentum vectors. The large vertical arrow represents the total angular momentum, the smallest arrow represents the orbit angular momentum, which has an angle i with the total angular momentum, and the other arrow represents Alpha's angular momentum, which has an angle δ with the total angular momentum. Beta's angular momentum is too small to show here.

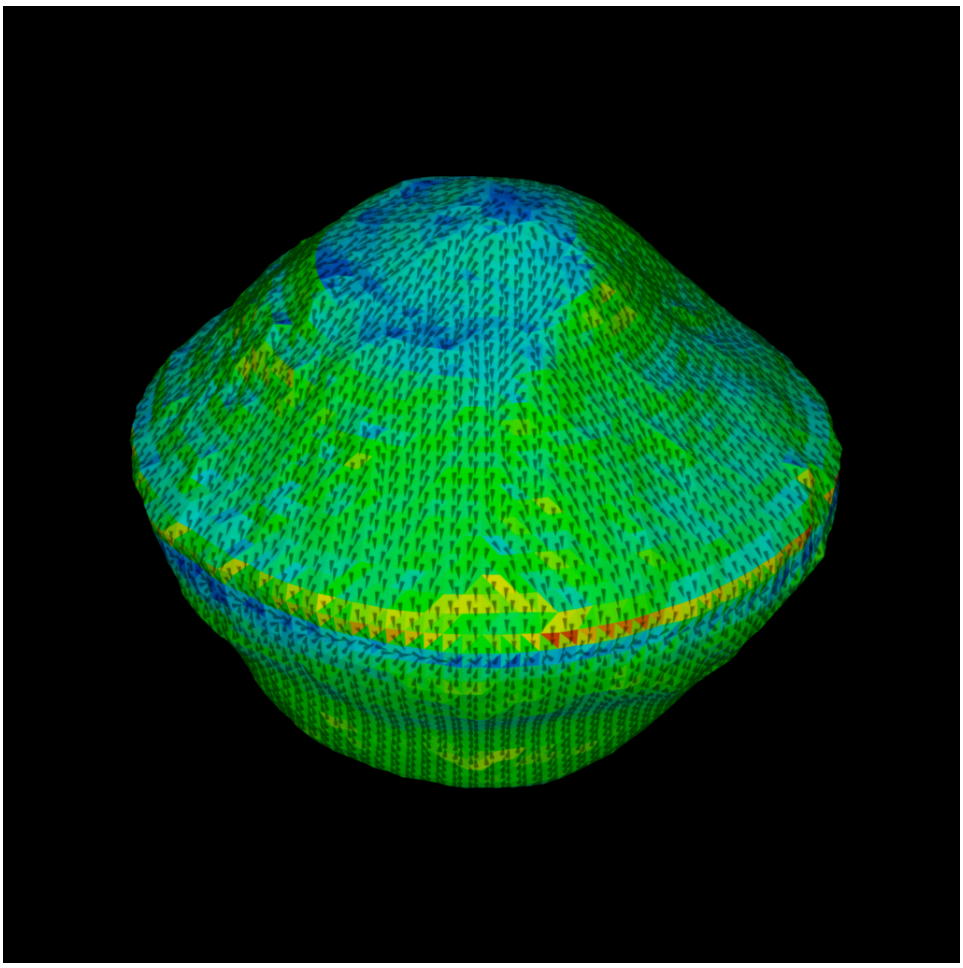

Figure S2: Effective gravitational slopes on Alpha with arrows pointing in the direction of steepest descent. The natural flow direction from both Northern and Southern hemispheres is towards the equator. Slopes range from zero (blue) to 70° (red).

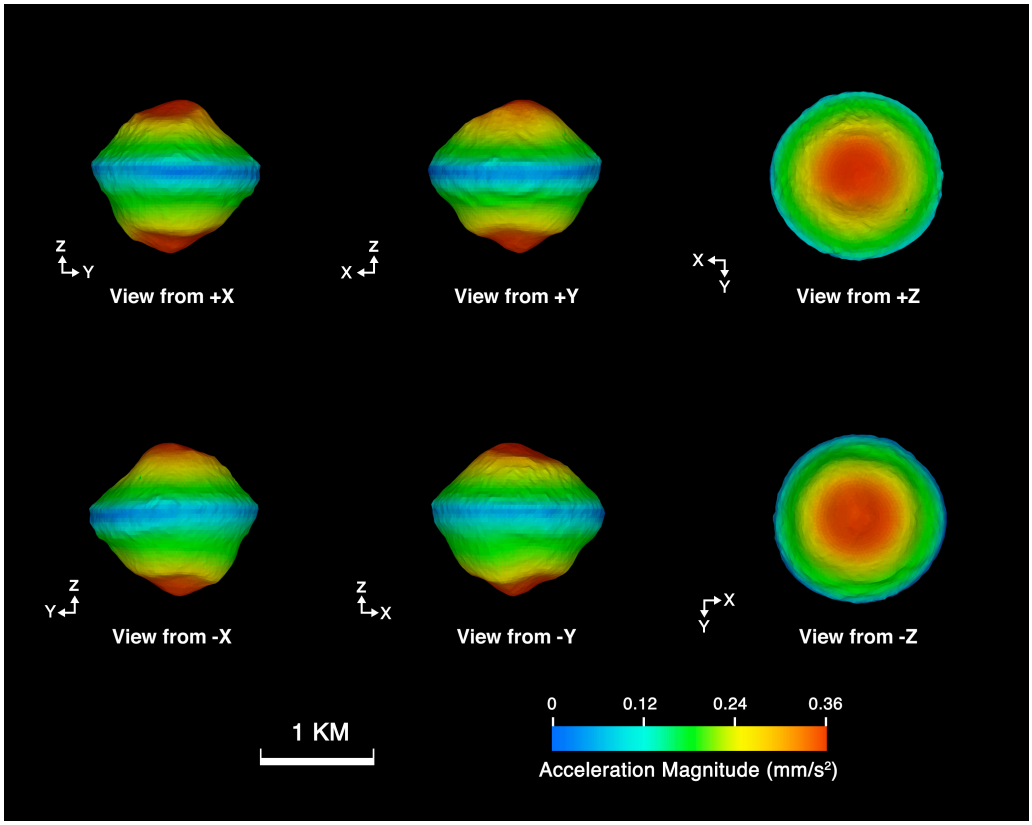

Figure S3: Surface acceleration on Alpha. Note the near vanishing of acceleration along the equator.

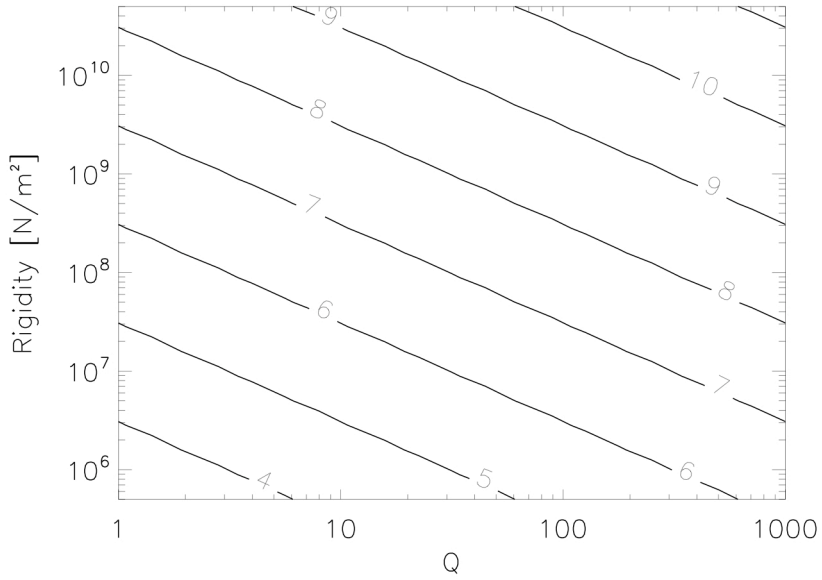

Figure S4: Logarithm of the timescale for tidal evolution in years as a function of tidal dissipation factor Q and rigidity μ. The timescales represent the time for the system to reach its current orbital separation under the influence of tides raised on Alpha by Beta.